REGIONAL BRAIN ATROPHY AND FUNCTIONAL DISCONNECTION ACROSS ALZHEIMER'S DISEASE EVOLUTION

Tommaso Gili, Mara Cercignani, Laura Serra, Roberta Perri, Federico Giove, Bruno Maraviglia, Carlo Caltagirone, Marco Bozzali

REGIONAL BRAIN ATROPHY AND FUNCTIONAL DISCONNECTION ACROSS ALZHEIMER'S DISEASE EVOLUTION

T Gili[1,2], M Cercignani[2], L Serra[2], R Perri[3], F Giove[1], B Maraviglia[1], C Caltagirone[3,4], M Bozzali[2].

[1]Marbilab, Enrico Fermi Center, Via Ardeatina 306, 00179 Rome, Italy.

[2]Neuroimaging Laboratory, Santa Lucia Foundation, IRCCS, Via Ardeatina 306, 00179 Rome, Italy.

[3]Department of Clinical and Behavioral Neurology, Santa Lucia Foundation, IRCCS, Via Ardeatina 306, 00179 Rome, Italy.

[4]Department of Neuroscience, University of Rome 'Tor Vergata', Via Mont Pelier 1, 00133-Rome, Italy.

Correspondence to: Dr. Marco Bozzali, Via Ardeatina 306, 00179 Rome, Italy. Telephone number: #39-06-5150 1324; Fax number: #39-06-5150 1213; E-mail address: m.bozzali@hsantalucia.it

Text word count=3803

Key words: AD; MCI; fMRI; Resting State, Functional Connectivity; VBM.

Abstract

Objective: to assess the contribution of regional grey matter (GM) atrophy and functional disconnection in determining the level of cognitive decline in patients with Alzheimer's disease (AD) at different clinical stages.

Methods Ten patients with amnesic mild cognitive impairment (a-MCI), 11 patients with probable AD, and 10 healthy controls were recruited. T1-volumes were obtained from each subject and post-processed according to an optimized voxel based morphometry protocol. Resting-state functional MRI data were also collected from the same individuals, and analysed to produce connectivity maps after identification of the default mode network (DMN) by independent component analysis (ICA).

Results*:* Compared to healthy controls, both AD and a-MCI patients showed a similar regional pattern of brain disconnection between the posterior cingulate cortex (PCC) and the medial prefrontal cortex (mPFC) and the rest of the brain. Conversely, the distribution of GM atrophy was significantly more restricted in a-MCI than in AD patients. Interestingly, the PCC showed reduced connectivity in a-MCI patients in the absence of GM atrophy, which was, in contrast, detectable at the stage of fully developed AD.

Conclusions*:* This study indicates that disconnection precedes GM atrophy in the PCC, which is a critical area of the DMN, and supports the hypothesis that GM atrophy in specific regions of AD brains likely reflect a long-term effect of brain disconnection. In this context, our study indicates that GM atrophy in PCC accompanies the conversion from MCI to AD.

Introduction

The clinical presentation of Alzheimer's disease (AD) is typically characterized by an early and prominent impairment of memory functions, followed by a progressive accumulation of additional cognitive deficits, eventually resulting in dementia[1]. A number of structural and functional neuroimaging studies have independently shown inconsistent distributions between structural[2-4] and metabolic changes[5-8] in AD brains. Only recently, brain volumetrics and Positron Emission Tomography (PET) were used in combination[9 10], showing that hypometabolism largely exceeds grey matter (GM) atrophy in most brain regions of AD patients[9]. Moreover, a strict relationship between hypometabolism in the posterior cingulate cortex (PCC), hippocampal volume, and disruption of the cingulum bundle was observed[10]. These findings suggest that the clinical manifestations of AD are not only associated with regional GM loss, but may also be due to abnormal functional integration of different brain regions. Functional MRI (fMRI) has shown the ability to record spontaneous brain activity fluctuations when subjects lie still in the scanner, at rest. The so-called default-mode network (DMN), which includes the PCC, inferior parietal, and medial prefrontal cortex (mPFC) has been identified as a neuronal network showing a coherent pattern of activation (functional connectivity)[11]. These regions, which show correlation in their spontaneous fluctuations at rest, are believed to be similarly modulated by cognitive tasks. In this perspective, changes in strength of correlation within regions of the DMN at rest, are expected to express an indirect measure of regional brain disconnection. Voxel-based morphometry (VBM) is a spatially-specific and unbiased method of analysis of MR images reflecting the regional GM volume at a voxel scale[12]. This technique has already been successfully applied to AD, showing patterns of GM abnormalities that fit well with the clinical stage of the disease, and also predict the risk of conversion from mild cognitive impairment (MCI)[13], which is a condition associated with an high risk of

conversion to AD in short time, to AD[14 15].

Aim of this study was to investigate, using VBM and resting-state fMRI, the contribution of regional GM atrophy and DMN disconnection in determining the level of cognitive decline in patients with AD at different clinical stages. For this purpose, three different groups of subjects were investigated, including healthy elderly individuals, patients with amnesic MCI (a-MCI), and patients with AD.

Materials and methods

Subjects. Ten patients meeting the diagnostic criteria for MCI[1] and 11 patients with a diagnosis of probable AD[16] attending a specialist dementia clinic were recruited for this study. All a-MCI patients complained of subjective memory loss, with no impact on their daily living activities, which was confirmed by an informant assistant. None of them fulfilled NINCDS-ADRDA consensus criteria[16] for the diagnosis of probable AD, and their Clinical Dementia Rating[17] (CDR) score did not exceed 0.5. Ten healthy subjects (HS), with no complaint of cognitive problems or any evidence of cognitive deficits on neuropsychological testing, were also enrolled in the study and served as control group. The principal demographic data of the studied population are summarized in Table 1. All recruited subjects (patients and controls) underwent an extensive neuropsychological battery testing for several cognitive domains (see below). Inclusion criteria required that a-MCI patients scored outside the range of normality (<95% of the lower tolerance limit of the distribution from the Italian normative data) in at least one of the memory tests, and performed within the normality cut-off scores in all other cognitive domains, and that HS did not score outside the normal range on any of neuropsychological tests (see below).

Subjects with either two or more hyperintense lesions with a 10 mm diameter or more than eight hyperintense lesions with a diameter between 5 to 9 mm on dual-echo MR

images were excluded. Indeed, the presence of vascular pathology might be at least partially responsible for cognitive deficits, making the diagnosis of MCI (on a neurodegenerative basis) or AD less plausible, as well as the condition of normality in healthy controls.

Major systemic, psychiatric and other neurological illnesses were carefully investigated and excluded in all studied subjects.

Ethics Committee approval from Santa Lucia Foundation (Prot. CE/AG4/PROG.198-84) and written informed consent (either from the subjects or from their responsible guardians if incapable) were obtained before study initiation.

Patients with a-MCI underwent a clinical and neuropsychological re-assessment (using the same battery employed at baseline) at one year follow-up. Then, they were reclassified in 3 groups: subjects who still had a purely amnesic form of MCI, those who developed multi-domain MCI, and those who converted to dementia.

Neuropsychological assessment. The extensive neuropsychological battery used to assess all recruited subjects included a general cognitive evaluation, using the Mini Mental State Evaluation (MMSE)[18 19], and tests specific for each cognitive domain: 1) Verbal episodic long-term memory: Immediate and Delayed recall of a 15-Word List[20], Short Story Recall[21]; 2) Visuo-spatial episodic long-term memory: Delayed recall of Complex Rey's Figure[22]; short-term memory: Digit span and Corsi Block Tapping task[23]; 3) Language: Naming subtest of Aachener Aphasia test[24]; 4) Problem-solving: Raven's Coloured Progressive Matrices[20]; 5) Executive functions and attention: Phonological Word Fluency[20], Categorical Word Fluency[21], Trail Making Test[25] and the Attentive Matrices[21]; 6) Praxis: Copy of drawings[21], Copy of Complex Rey's Figure[22].

MRI acquisition. All subjects underwent an MRI examination, obtained at 3 T (Magnetom Allegra, Siemens, Erlangen, Germany), including the following sequences: 1) dual-echo turbo spin echo [TSE] (TR=6190 ms, TE=12/109 ms, matrix=256x192,

FOV=230x172.5, 48 contiguous slices, slice thickness=3 mm, total scan time=4 minutes); 2) 3D Modified Driven Equilibrium Fourier Transform (MDEFT) scan (TR=1338 ms, TE=2,4 ms, TI=910 ms, flip angle=15°, Matrix=256x224x176, in-plane FOV=256x224 mm^2, slice thickness=1 mm, total scan time=12 minutes); 3) T2*-weighted EPI sensitized to BOLD contrast (TR=2080 ms, TE=30 ms, 32 axial slices parallel to AC-PC line, matrix=64x64, pixel size =3x3 mm 2, slice thickness=2.5 mm, flip angle=70°) for resting state fMRI. BOLD EPI images were collected during rest for a 7-min and 20-sec period, resulting in a total of 220 volumes. During this acquisition, subjects were instructed to keep their eyes closed, not to think of anything in particular, and not to fall asleep.

FMRI data analysis. All steps of this analysis are schematically reported in Figure 1. Resting state fMRI data were pre-processed using statistical parametric mapping (Wellcome Department of Imaging Neuroscience; SPM5), and in-house software implemented in Matlab (the MathWorks, Inc.). For each subject the first five volumes of the fMRI series were discarded to allow for T1 equilibration effects. The pre-processing steps included correction for head motion, compensation for slice-dependent time shifts and registration to the T1- weighted high resolution image (SPM5). The functional data were passed through an additional series of processing steps. Several sources of non specific spurious variance were adjusted by including the following factors as nuisance covariates in the regression model: the six parameters obtained by rigid body head motion correction; the signal averaged over whole brain voxels; the signal averaged over cerebral spinal fluid (CSF) voxels; the signal averaged over white matter (WM) voxels. CSF and WM voxels were derived from the correspondent masks obtained by the VBM pre-processing (see below). Then, for each voxel of the fMRI data, temporal filtering was applied to remove constant offsets and linear trends over each run, while retaining frequencies in the 0.009-0.08 Hz band. Data were then normalized into

Montreal Neurological Institute (MNI) space coordinates[26] and smoothed using a 8-mm full-width at half-maximum (FWHM) Gaussian kernel. In the present work, we employed the independent component analysis (ICA) (Group ICA for fMRI toolbox, GIFT, http://icatb.sourceforge.net/) to identify, on a subject by subject basis, regions belonging to the DMN, as previously described[27-30]. Briefly, Group ICA for fMRI toolbox first concatenates the individual data across time, and then produces a computation of subject specific components and time courses. For all subjects grouped together, the toolbox performed the analysis in three steps: (1) data reduction, (2) application of the FastICA algorithm, and (3) back-reconstruction for each individual subject[31]. As expected, the functionally relevant resting state networks included the DMN, characterized by the synchronous oscillation of the PCC, the lateral and mPFC, and the parietal cortex[11 29-31]. Figure 2 (top panel) illustrates the average result obtained by ICA in all subjects. In the estimation of within network variations of functional connectivity we focused on the two regions that showed the highest peak Z-score in the mean spatial map obtained from all subjects together (Z>5), the PCC and mPFC. Then, in each subject scan, we identified these two regions-of-interest (ROIs) by considering, for each of them, a cluster including the 100 voxels that obtained the highest score in each ICA-driven DMN. Finally, these regions were used for the correlation analysis between the DMN and the rest of the brain as previously described[32 33].

The signal time course of each of the two selected ROIs (belonging to the DMN) was correlated with all voxels included in the brain, thus obtaining correlation maps[34], which highlighted those brain regions intrinsically correlated with the ROIs themselves. The basic procedure[33] consisted of computing for each brain voxel the correlation coefficient against the BOLD time series extracted from each considered ROI (seed region). Each correlation map was then converted to normally distributed Z values using Fisher's r-to-Z transformation. As explained below, the correlation maps were used for group

analyses.

VBM analysis**.** The T1-weighted volumes (MDEFT) were pre-processed using the VBM protocol implemented in SPM5, which consists of an iterative combination of segmentations and normalisations to produce a GM probability map[35] in MNI space for each subject. The templates used for VBM analysis are those provided with SPM5. In order to compensate for compression or expansion which might occur during warping of images to match the template, GM maps were "modulated" by multiplying the intensity of each voxel in the final images by the Jacobian determinants derived from the spatial normalization step[36]. Every subject's GM, WM and CSF volumes were recorded for further analysis. All data were then smoothed using a 12-mm FWHM Gaussian kernel. As explained in the next section, modulated and smoothed GM maps were used for group analyses.

Voxelwise statistics for resting state fMRI and VBM. PCC and mPFC driven Z-score maps were respectively included in two second level full factorial statistical analyses in SPM5. Age, education and total GM volumes were entered as covariates of no interest. For each analysis (PCC and mPFC driven Z-score maps), an F-contrast ($p=0.001$) was first performed to assess the global pattern of changes across all groups (effects of interest). Then, within the whole pattern of functional changes, between groups T-contrasts were used to assess the distribution of functional changes at the stages of a-MCI and AD (post-hoc analyses). In all T contrasts (AD vs. HS; aMCI vs. HS; aMCI vs. AD) changes were considered as statistically significant at p values<0.001 cluster level uncorrected, corresponding to a minimum cluster size of 10.

In VBM analysis, in order to assess the evolution of regional GM atrophy during the entire AD course and at the early stage (a-MCI), voxelwise statistics was performed using the same model employed for the analysis of functional maps. Age, education and

intra-cranial volume (ICV=GM volume+WM volume+CSF volume) were entered as covariates of no interest.

This use of ICV as a covariate of no interest has been previously used in VBM studies[14,37] in patients with AD and MCI. ICV is expected to correct for the potential bias due to inter-subject variability in head size without affecting the sensitivity of VBM to detect regional GM changes (effects of interest). Consistently with fMRI analyses, we first performed an F-contrast across groups (p=0.0005), thus obtaining the whole pattern of regional GM changes. Then, we investigated (within such a pattern) the structural changes which were present in patients with AD as compared to HS by performing a between groups T-contrast (post-hoc analysis). Our small sample size was insufficient to detect in a whole brain analysis GM changes at a corrected level between a-MCI patients and the other two groups (HS and AD). Thus, we decided to restrict the analysis to four strategic regions: the right and left hippocampus, the PCC and the mPFC. Coordinates to select these anatomical locations were taken from the maxima of the correspondent clusters obtained by an F-contrast across all groups (p=0.0005). Spherical regions of interest (diameter=12mm) were then defined, and the following between groups T-contrasts were performed using a small volume correction: a-MCI vs. HS; a-MCI vs. AD (statistical threshold: p values family wise error corrected at voxel level <0.05). This small volume correction analysis has the advantage to be highly specific. Indeed, for the purposes of this study, it is critical to learn with a high confidence level whether specific brain regions of reduced connectivity are still structural preserved at the stage of a-MCI.

Results

Demographic characteristics. There were no differences between a-MCI and AD patients with respect to age, gender and education, while HS were younger and more

educated than patients. As already mentioned, age and education were included in all neuroimaging analyses as covariates of no interest.

Neuropsychological evaluation at baseline**.** Groups performances obtained at all neuropsychological tests administered at baseline, are summarized in Table 2. The mean MMSE scores (corrected for education) were different between all groups ($p<0.001$, one-way ANOVA). A statistical group comparison showed that a-MCI patients performed worse than HS at all memory tests (p values<0.05). Moreover, they reported significantly lower scores than HS at the Phonological verbal fluency and Categorical fluency tests (p values<0.05), although their performance was within the range of normality, as defined above. Patients with AD compared to HS reported a widespread impairment of all the cognitive functions explored ($p<0.05$), including long and short term memory, executive functions, praxis abilities, language abilities and reasoning.

Clinical and neuropsychological follow-up At one year follow-up, 3 out of 10 a-MCI patients remained stable (30%) from a clinical and neuropsychological point of view, 3 out of 10 had developed a multi-domain MCI (30%), and 4 out of 10 had converted to dementia (40%).

Resting State fMRI. In Figure 2 (bottom panel) there are illustrated, for each z-map (respectively generated from PCC and mPFC), the main patterns of functional connectivity obtained in each studied group (HS, a-MCI and AD patients).

Figure 3 (top panel, right side) illustrates the patterns of functional changes, respectively obtained using PCC and mPFC driven z-maps, in AD patients as compared to HS. For the most relevant regions, Figure 3 (bottom panel) reports also plots showing mean (SD) values for each studied group (HS, a-MCI, AD).

Table 3 summarizes, for each analysis (z-maps respectively generated from PCC and mPFC), those brain regions presenting with significant changes in connectivity between groups.

When comparing patients with AD to HS, PCC showed a significant reduction of functional connectivity with the parahippocampal gyrus, the posterior and anterior cingulate, the superior frontal gyrus and the precuneus bilaterally. Reduced connectivity was also present within the left orbitofrontal cortex. In its turn, the mPFC, showed significantly reduced connectivity with the anterior cingulate and superior frontal gyrus bilaterally, and with the left orbitofrontal cortex and posterior cingulate.

A-MCI patients compared to HS showed a bilateral reduction of connectivity in the anterior cingulate and superior frontal gyrus, by considering either the PCC- or the mPFC-driven analysis. The mPFC-driven analysis revealed also an additional area of reduced connectivity in the posterior cingulate. The direct comparison between a-MCI and AD patients revealed a decrease of functional connectivity in the posterior cingulate cortex of the latter group in both analyses (PCC- and mPFC-driven), and in the parhaippocampal gyri in the PCC-driven analysis only.

VBM. None of the T1 weighted volumes of the participants were affected by macroscopic artefacts, as assessed by visual examination. As expected, AD patients compared to HS showed a widespread pattern of regional GM reduction, including the temporal and parietal lobes, the precuneus, the insular and the prefrontal cortex (See Table 4). Some of these regions relevant for the purposes of the study are also illustrated in Figure 3 (top panel, left side), together with plots showing mean (SD) values for each studied group (HS, a-MCI, AD) (bottom panel).

We also investigated the degree of regional GM atrophy in a-MCI patients as compared to both, HS and AD patients, using a small volume correction analysis. These results are summarized in Table 4. Patients with a-MCI compared to HS showed a significant reduction of regional GM volumes in the hippocampus and mPFC bilaterally (p corrected <0.05), but not in the PCC/precuneus. In contrast, they showed increased GM

volumes in the PCC/precuneus (p corrected <0.05), but not in the hippocampi and mPFC when compared to patients with AD.

Discussion

The current study combines functional and structural MRI to quantify the relative role played by regional GM atrophy over the transitional stage between normal aging and dementia, by considering a-MCI as an early clinical stage of AD. Although this last assumption was not fully verified in all recruited patients with a-MCI, the clinical-neuropsychological follow-up at 1 year demonstrated a conversion to AD in 40% of them, and accumulation of additional impairments in cognitive domains other than memory in another 30 %. This indicates that our a-MCI group may be regarded, at least in a relevant part, as including patients "in a prodromal stage of AD", as defined by some authoritative authors[1].

Specific patterns of structural and functional changes were identified within the DMN, with a different expression associated with an early (a-MCI) and with an advanced stage of the disease (fully developed dementia). Our functional investigation was focused on assessing changes of brain connectivity as a function of AD evolution between two regions of the DMN, which were automatically identified using ICA, and the rest of the brain. As for functional data analysis, regional patterns of GM atrophy were also detected in a data driven fashion, using VBM.

VBM analysis returned patterns of GM atrophy which are consistent with previous literature, with a widespread involvement of association cortices in demented patients[4 15], and a more confined subset of atrophic regions in patients with a-MCI[15]. For the purposes of this study, we mainly focussed on those brain regions in which GM atrophy and functional disconnection showed anatomical overlap in patients with fully developed dementia as compared to HS. Then, we investigated functional and structural

changes across AD evolution, by comparing a-MCI with AD patients and HS. The PCC revealed the presence of functional disconnection with the anterior cingulate and superior frontal gyrus as a feature of the a-MCI stage, even in the absence of a (detectable) local GM loss within the PCC/precuneus. In this latter region, we were unable to find significant GM changes between a-MCI patients and HS even restricting the analysis to a small volume of interest (Table 4). Consistently, but in opposite direction, PFC showed a reduced connectivity with PCC in patients with a-MCI. These findings are consistent with a large body of literature that, using PET, has consistently demonstrated a reduction of metabolism in the PCC of patients with early AD[3 5-10], in the absence of a remarkable atrophy[9 10]. It has been suggested by many authors that this posterior hypometabolism is likely to express a reduction of neuronal afferents from medial temporal lobes to PCC, mainly due to hippocampal atrophy[38]. According to our data, the local atrophy of the medial temporal lobes is equally present in both patients groups, AD and a-MCI (Figure 3, plot 3). As expected, there is a pattern of functional disconnection between the parahippocampi and regions of the DMN which is already remarkable at the stage of a-MCI. However, it is only in AD patients that this correlation is completely lost, as suggested by its negative trend (Figure 3, plot 6). All these data are consistent with a recent study that provided a direct evidence supporting disconnection as a major factor that contributes to the posterior hypometabolism in patients with early AD[10]. In this perspective, our results help to further elucidate the differential role of disconnection and GM atrophy in the PCC, the latter occurring only at more advanced stages of the disease. As further discussed below, this evolution of brain tissue abnormalities in the PCC from functional to structural changes might be critical for the clinical conversion from a-MCI to AD. The pattern of GM atrophy we observed in a-MCI patients involves also the medial prefrontal cortex bilaterally. Hippocampus and medial prefrontal cortex are regions structurally connected to each

other through the cingulate bundle, and they are both involved, at different level, in memory processing[39 40], the only function that was frankly impaired in our cohort of a-MCI patients.

We might speculate that the reduced connectivity found in the PCC of a-MCI patients is not only associated with hippocampal atrophy, but also with the GM loss observed in frontal regions, which are also connected to the PCC by the cingulate bundle. This suggests that the hippocampus is not the only structure responsible for PCC abnormalities in AD evolution. PCC is believed to be one of the key nodes of the so called DMN, whose disruption has been demonstrated not only to be present in AD patients[28], but also to correlate with global measures of cognitive decline[30]. We further argue that the late atrophy of the PCC/precuneus, which follows an early reduction of functional connectivity, may be crucial for the clinical conversion from a-MCI to multi-domain MCI, and finally to fully developed dementia. In this perspective, the PCC would represent not only an early diagnostic marker of AD[28], but also a potential marker of conversion from MCI to AD[41].

The approach used in the current study seems to be particularly promising in clarifying the patho-physiology of AD evolution. However, it should be noted that voxels compared in VBM versus those compared in resting state fMRI analysis are in the same anatomical regions but overlap only partially, and that different statistical thresholds were used for the two datasets. Therefore, a direct comparison of structural and functional data should be viewed with caution. The method of analysis could indeed be improved by developing a specific technique for cross-modality imaging comparisons (in this case, functional and structural).

The main limitations lie in the small sample size, and in age and education differences between patients and controls. We tried to minimize the impact of small sample size by

including a very well selected sample of patients with a-MCI. Moreover, we included age and education as covariates of no interest in all imaging analyses. Nevertheless, further studies are needed to confirm our results, and to extend the investigation to larger populations, possibly including subgroups of patients at different level of cognitive impairment. Finally, we gave a longitudinal interpretation of our results (i.e. decreased connectivity in PCC precedes GM atrophy in AD evolution) on the basis of a theoretical model which considers AD as a continuum of cognitive decline between normal aging and dementia, with a-MCI as a prodromal stage of the disease. However, we should reiterate that the current study has employed a cross-sectional design, and our findings need be confirmed by further longitudinally-based studies.

Acknowledgments

The authors thank Dr. Emiliano Macaluso for his help with data analysis.

Competing interests

The authors declare that they have no actual or potential conflicts of interest.

Founding

This project has been supported by grants of the Italian Ministry of Health and of the Italian Ministry of University and Research.

References

1. Petersen RC, Morris JC. Conceptual overview. In: Petersen RC, eds. Mild Cognitive Impairment: Aging to Alzheimer's Disease. Oxford University Press, New York 2003:1-14.

2. Baron JC, Chételat, G, Desgranges B, et al. In vivo mapping of gray matter loss with voxel-based morphometry in mild Alzheimer's disease. Neuroimage 2001;14:298-309.

3. Matsuda H, Kitayama N, Ohnishi T, et al. Longitudinal evaluation of both morphologic and functional changes in the same individuals with Alzheimer's disease. J Nucl Med 2002;43:304-11.

4. Karas GB, Burton EJ, Rombouts SA, et al. A comprehensive study of gray matter loss in patients with Alzheimer's disease using optimized voxel-based morphometry. Neuroimage 2003;18:895-907.

5. Minoshima S, Giordani B, Berent S, et al. Metabolic reduction in the posterior cingulate cortex in very early Alzheimer's disease. Ann Neurol 1997;42:85-94.

6. Ibanez V, Pietrini P, Alexander GE, et al. Regional glucose metabolic abnormalities are not the result of atrophy in Alzheimer's disease. Neurology 1998;50:1585-93.

7. Nestor PJ, Fryer TD, Smielewski P, et al. Limbic hypometabolism in Alzheimer's disease and mild cognitive impairment. Ann Neurol 2003;54:343-51.

8. Borroni B, Anchisi D, Paghera B, et al. Combined 99mTc-ECD SPECT and neuropsychological studies in MCI for the assessment of conversion to AD. Neurobiol Aging 2006;27:24-31.

9. Chételat G, Desgranges B, Landeau, B, et al. Direct voxel-based comparison between grey matter hypometabolism and atrophy in Alzheimer's disease. Brain 2008; 131:60-71.

10. Villain N, Desgranges B, Viader F, et al. Relationships between hippocampal atrophy, white matter disruption, and gray matter hypometabolism in Alzheimer's disease. J Neurosci 2008;28:6174-81.

11. Raichle ME, Snyder AZ. A default mode of brain function: a brief history of an evolving idea. Neuroimage 2007;37:1083-90.

12. Good CD, Johnsrude IS, Ashburner J, et al. A voxel-based morphometric study of ageing in 465 normal adult human brains. Neuroimage 2001;14:21-36.

13. Petersen RC, Doody R, Kurz A, et al. Current concepts in mild cognitive impairment. Arch Neurol 2001;58:1985-92.

14. Chételat G, Landeau B, Eustache F, et al. Using voxel-based morphometry to map the structural changes associated with rapid conversion in MCI: a longitudinal MRI study. Neuroimage 2005;27:934-46.

15. Bozzali M, Filippi M, Magnani G, et al. The contribution of voxel-based morphometry in staging patients with mild cognitive impairment. Neurology 2006;67:453-60.

16. McKhann G, Drachman D, Folstein M, et al. Clinical diagnosis of Alzheimer's disease: report of the NINCDS-ADRDA Work Group under the auspices of Department of Health and Human Services Task Force on Alzheimer's Disease. Neurology 1984;3:939-44.

17. Hughes CP, Berg L, Danziger WL, et al. A new clinical scale for the staging of dementia. Br J Psychiatry 1982;140,566-72.

18. Folstein MF, Folstein SE, McHugh PR. "Mini-mental state". A practical method for grading the cognitive state of patients for the clinician. J Psychiatr Res 1975;12:189-98.

19. Measso G, Cavartezan F, Zappalà G, et al. The Mini Mental State Examination: Normative study of a random sample of Italian population. Dev Neuropsychol 1993;9:77-85.

20. Carlesimo GA, Caltagirone C, Gainotti G . The mental Deterioration Battery: normative data, diagnostic reliability and qualitative analyses of cognitive impairment. The group of the Standardization of the Mental Deterioration Battery. Eur Neurol 1996;36:378-84.

21. Spinnler H, Tognoni P. Standardizzazione e taratura italiana di test neuropsicologici. Ital J Neurol Sci 1987;Suppl 8.

22. Carlesimo GA, Boccione I, Fadda L, Graceffa A, et al. Standardizzazione di due test di memoria per uso clinico: Breve Racconto e Figura di Rey. Nuova Rivista di Neurologia 2002;12:3-13.

23. Orsini A, Grossi D, Capitani E, et al. Verbal and spatial immediate memory span: Normative data from 1355 adults and 1112 children. Ital J Neurol Sci 1987;8:539-48.

24. De Blese R, Denes G, Luzzatti C, et al. L'Aachener Aphasie test I: problemi e soluzioni per una versione italiana del test e per uno studio crosslinguistico dei disturbi afasici. Archivio di Psicologia, Neurologia e Psichiatria 1996;47:209-36.

25. Giovagnoli AR, Del Pesce M, Mascheroni S, et al. Trail making test: normative values from 287 normal adult controls. Ital J Neurol Sci 1996;17:305-9.

26. Evans AC, Collins DL, Mills SR, et al. 3D statistical neuroanatomical models from 305 MRI volumes. Proc. IEEE-Nuclear Science Symposium and Medical Imaging Conference 1993;1813-17.

27. Calhoun VD, Adali T, Pearlson GD, et al. A method for making group inferences from functional MRI data using independent component analysis. Hum Brain Mapp 2001;14:140-51.

28. Greicius MD, Srivastava G, Reiss AL, et al. Default-mode network activity distinguishes Alzheimer's disease from healthy aging: Evidence from functional MRI. Proc Natl Acad

Sci USA 2004;101:4637-42.

29. Damoiseaux JS, Rombouts SA, Barkhof F, et al. Consistent resting-state networks across healthy subjects. Proc Natl Acad Sci USA 2006;103:13848-53.

30. Sorg C, Riedl V, Muhlau M, et al. Selective changes of resting-state networks in individuals at risk for Alzheimer's disease. Proc Natl Acad Sci USA 2007;104:18760-5.

31. De Luca M, Beckmann CF, De Stefano N, et al. fMRI resting state networks define distinct modes of long-distance interactions in the human brain. Neuroimage 2006;29:1359-67.

32. Biswal B, Yetkin FZ, Haughton VM, et al. Functional connectivity in the motor cortex of resting human brain using echo-planar fMRI. Magn Res Med 1995;34:537-41.

33. Fox MD, Snyder AZ, Vincent JL, et al. The human brain is intrinsically organized into dynamic, anticorrelated functional networks. Proc Natl Acad Sci USA 2005;102:9673-8.

34. Vincent JL, Snyder AZ, Fox MD, et al. Coherent spontaneous activity identifies a hippocampal-parietal memory network. J Neurophysiol 2006;96,3517-31.

35. Ashburner J, Friston KJ. Unified segmentation. Neuroimage 2005;26:839-51.

36. Ashburner J, Friston KJ. Why voxel-based morphometry should be used. Neuroimage 2001;14:1238-43.

37. Serra L, Cercignani M, Lenzi D, et al. Grey and white matter changes at different stages of Alzheimer's disease. J Alzheimers Dis 2010;19:147-59.

38. Buckner RL. Memory and executive function in aging and AD: multiple factors that cause decline and reserve factors that compensate. Neuron 2004;44:195-208.

39. Frey S, Petrides M. Oritofrontal cortex and memory formation. Neuron 2002;36:171-6.

40. Davachi L, Mitchell JP, Wagner AD. Multiple routes to memory: distinct medial temporal lobe processes build item and source memories. Proc Natl Acad Sci USA 2003;100:2157-

62.

41. Wang K, Liang M, Wang L, et al. Altered functional connectivity in early Alzheimer's disease: a resting-state fMRI study. Hum Brain Mapp 2007;28, 967-78.

Figure legends

Figure 1. The figure shows the processing pipeline of resting state functional connectivity analysis. Group Independent Component Analysis (ICA) was first used to concatenate individual fMRI data across time, thus producing, for each subject, a computation of components and time courses (back reconstruction). From the functionally relevant components, we identified, subject by subject, the default mode network (DMN), which is characterized by the synchronous oscillation of the posterior cingulate cortex (PCC), the lateral parietal and medial prefrontal cortex (mPFC). The two regions showing the highest peak z-score in the mean spatial map, namely the PCC and the mPFC, were chosen as regions-of-interest (ROIs) to produce, subject by subject, maps for the correlation analysis. In each subject, these two ROIs were defined by limiting each of them to those 100 voxels which reported the highest score in the ICA-driven DMN. Finally, each ROI was used to produce correlation maps between voxels in the PCC and mPFC and all the remaining voxels of the brain, thus producing, for each subject, the correspondent PCC- and mPFC -driven correlation maps. Each correlation map was then converted to normal z values using Fisher's r-to-z transformation, and used for statistical group analyses.

Figure 2. Top panel illustrates the mean spatial independent component (IC) pattern obtained from all subjects during resting state. Blue arrows indicate the two regions (posterior cingulate [PCC] and medial prefrontal cortex [mPFC]) with the highest Z peak, which were selected as regions of interest (ROIs) for subsequent correlation analysis. Bottom panel shows, for each studied group (HS, a-MCI and AD patients), results of correlation analysis obtained using the PCC (left) and the mPFC ROI (right)

to produce connectivity maps. All functional results are superimposed on a high resolution single-subject T1-weighted volume template.

See text for further details.

Figure 3. Distribution of reduced regional GM volume (top panel on the left) and functional connectivity (top panel on the right) observed in patients with fully developed dementia (AD) as compared to healthy subjects (HS). Changes of functional connectivity were assessed using both PCC- and mPFC-driven connectivity maps. In all cases, the T-contrasts were performed by masking them with the global effect across groups assessed by F-contrast. Statistical thresholds are the same used in tables 3 and 4. For some relevant regions, the correspondent mean (SD) values are plotted for the three studied groups (bottom panel).

See text for further details.

Table 1. Principal demographic and clinical characteristics of studied subjects.

	a-MCI patients **n=10**	**AD patients** **n=11**	**HS** **n=10**
Sex, F/M	4/6	4/7	3/7
Mean age (SD), years	71.2 (4.1)*	71.9 (7.9)**	64.1 (10.5)
Mean education (SD), years	10.9 (5.3) *	9.9 (4.9) **	14.3 (3.4)

Abbreviations: AD= Alzheimer's disease; a-MCI= amnesic mild cognitive impairment; HS=healthy subjects. * $p<0.05$ a-MCI *vs*. HS; ** $p<0.05$ AD *vs*. HS.

Table 2 Neuropsychological assessment of studied subjects.

Cognitive function	Neuropsychological Test (cut-off score)	Mean (SD) scores		
		a-MCI	**AD**	**HS**
Global measure				
	Mini Mental State Examination (≥23.8)	25.1 (1.2)#	19.7 (4.5)*§	28.34 (2.0)
Long term memory				
Verbal episodic	**15 Rey's words list (Immediate recall)** (≥28.5)	32.0 (5.4)#	20.4 (9.2)*§	45.2 (9.4)
	15 Rey's words list (Delayed recall) (≥4.7)	4.7 (2.6)#	0.5 (1.2)*§	10.0 (2.3)
	Story recall (≥2.39)	4.9 (3.8)#	2.5 (2.9)*§	11.1 (1.9)
Visuo-spatial episodic	**Rey's Complex Figure (**Delayed recall) (≥6.3)	8.8 (5.0)#	0.3 (1.0)*§	15.0 (8.2)
Short term memory				
	Digit span (≥3.7)	5.2 (0.8)	4.7 (1.1)*	6.0 (1.2)
	Corsi Block tapping task (≥3.5)	4.2 (1)#	3.4 (1.5)*	5.4 (0.6)
Language				

Naming	**Aachen Aphasie Test** (≥8.0)	9.0 (0.0)	7.3 (2.0)*§	9.0 (0.0)
Comprehension	**Token test** (≥26.5)	33.9 (1.9)	27.8 (5.9)*§	34 (1.9)
Reasoning				
	Raven's progressive matrices (≥18.9)	29.0 (3.0)	23.5 (5.6)*§	30.3 (4.2)
Executive functions				
	Attentional Matrices (≥31)	48.5 (6.3)	30.0 (15.0)*§	50.2 (4.3)
	Trail Making Test			
	Part A (≤94)	54.3 (16.4)	94.0 (57.8)*§	46.9 (9.1)
	Part B (≤283)	114.5 (47.0)	242.5 (112.6)	87.0 (60.0)
	Phonological verbal fluency (≥17.3)	27.1 (6.5)#	20.8 (12.7)*	37.4 (8.4)
	Categorial fluency (≥7.2)	13.0 (2.4)#	6.1 (3.9)*§	17.0 (2.4)
Praxis abilities				
	Copy of drawings (≥7.2)	13.5 (0.8)#	10.2 (2.2)*§	11.8 (1.2)

Abbreviations: AD= Alzheimer's disease; a-MCI= amnesic mild cognitive impairment; HS=healthy subjects.

*p<0.05 AD *vs* HS; § p<0.05 AD *vs* a-MCI; # p<0.05 a-MCI *vs* HS;

For each administered test appropriate adjustments for sex, age and education were applied according to the Italian normative data.

Cut-off scores of normality (≥95% of the lower tolerance limit of the normal population distribution) are also reported.

Table 3. Regional differences in functional connectivity between patients with a-MCI, AD, and HS.

	Side	Size	Coordinates (mm)			Peak Z-score
			x	y	z	
AD patients < HS						
PCC-driven functional connectivity						
Parahippocampal gyrus	R	71	34	-26	-18	3.91
Parahippocampal gyrus	L	49	-26	-18	-22	3.61
Orbito-frontal cortex	L	15	-28	16	-20	3.45
Anterior cingulate/superior frontal gyrus	B	34	0	48	16	3.28
Precuneous	B	35	-4	-72	28	3.29
Posterior cingulate cortex	B	11	0	-54	22	3.28
mPFC-driven functional connectivity						
Anterior cingulate/superior frontal gyrus	B	70	0	48	18	3.34
Posterior cingulate cortex	L	23	-16	-46	38	3.29
Orbito-frontal cortex	L	14	-30	14	-18	3.13
a-MCI patients < HS						
PCC-driven functional connectivity						
Anterior cingulate/superior frontal gyrus	B	122	2	46	14	3.60
mPFC-driven functional connectivity						
Anterior cingulate/superior frontal gyrus	B	17	2	46	30	3.18
Posterior cingulate cortex	B	16	4	-30	36	3.13
a-MCI > AD patients						
PCC-driven functional connectivity						

Posterior cingulate cortex	B	21	-4	-52	22	3.22
Parahippocampal gyrus	R	29	26	0	-24	3.21
Parahippocampal gyrus	L	10	-22	-16	-24	3.18
mPFC-driven functional connectivity						
Posterior cingulate cortex	B	11	-8	-24	3	3.30

Abbreviations: AD= Alzheimer's disease; a-MCI= amnesic mild cognitive impairment; HS=healthy subjects; PCC= posterior cingulated cortex; mPFC= medial prefrontal cortex; L=left; R=right; B=bilateral.

There are here reported regional changes in functional connectivity between all groups (a-MCI, AD, and HS). Between group comparisons (T-contrasts) were performed as post hoc analyses by masking them with the global effect estimated across all groups by F-contrast ($p=0.001$). Statistical threshold for T-contrasts was set to p values <0.001 at uncorrected level. Each region size is expressed in number of voxels. Only regions with a minimum size of 10 voxels have been considered as statistically significant. In all the areas where we found between-group differences, there was a positive correlation between the two regions in healthy controls. The reductions found in patients correspond to a reduction in the strength of correlation. The only two areas were there was an inversion in the sign of the correlation (from positive to negative) were the L and R parahippocampal gyri, in patients with AD.

See text for further details.

Table 4. Regional grey matter atrophy between patients with a-MCI, AD, and HS.

Brain region	Side	Size	Coordinates (mm)			Peak Z-score
			x	y	z	
AD patients < HS						
			Whole brain analysis			
Posterior cingulated cortex/Precuneous	B	1797	-6	-66	52	5.62
Inferior temporal gyrus	R	445	-50	-62	-18	5.38
Fusiform gyrus	R		-30	-86	-26	5.12
Orbitofrontal cortex	R	286	46	32	-14	5.03
Hippocampus	R	107	10	-2	-16	4.75
Hippocampus	L	78	-4	-4	-14	4.73
Angular gyrus	L	469	-64	-42	24	4.71
Medial frontal and orbital cortex	B	306	-4	54	-12	4.53
Orbitofrontal cortex	L	11	-44	30	-18	4.40
Insula	R	231	32	3	8	4.32
Insula	L	72	-30	6	6	4.33
a-MCI patients < HS						
			Small volume analysis			
Hippocampus	R	455	18	0	-16	3.16
Hippocampus	L	245	-8	0	-16	3.50
Posterior cingulated cortex/Precuneous	B	-	-6	-64	52	N.S.C.
Medial prefrontal and orbital cortex	B	575	-2	50	-12	3.71
a-MCI > AD patients						
			Small volume analysis			

Hippocampus	R	-	18	0	-16	N.S.C.
Hippocampus	L	-	-8	0	-16	N.S.C.
Posterior cingulate cortex/Precuneous	B	488	-6	-64	52	4.85
Medial prefrontal and orbital cortex	B	-	-2	50	-12	N.S.C.

Abbreviations: AD=Alzheimer's disease; HS=healthy subjects; R=right; L=left; B=bilateral; N.S.C.=no suprathreshold clusters.

There are here reported significant changes of regional grey matter (GM) volume between groups. The comparison between AD patients and HS was performed including the whole brain. The T-contrast was performed as a post hoc analysis (statistical threshold cluster level corrected < 0.001) by masking it with the global effect across all groups estimated by F-contrast (p=0.0005). The comparison between a-MCI patients and HS and AD patients, was performed using the small volume correction in four anatomical locations which are critical for the combination of functional and structural investigations. Coordinates for these anatomical locations were taken from the maxima resulting from the F-contrast across all groups (p=0.0005). Spherical regions of interest (diameter=12mm) were then defined, and the following between groups T-contrasts were performed: a-MCI vs. HS; a-MCI vs. AD (statistical threshold: p values family wise error corrected at voxel level <0.05). Each region size is expressed in number of voxels. See text for further details.

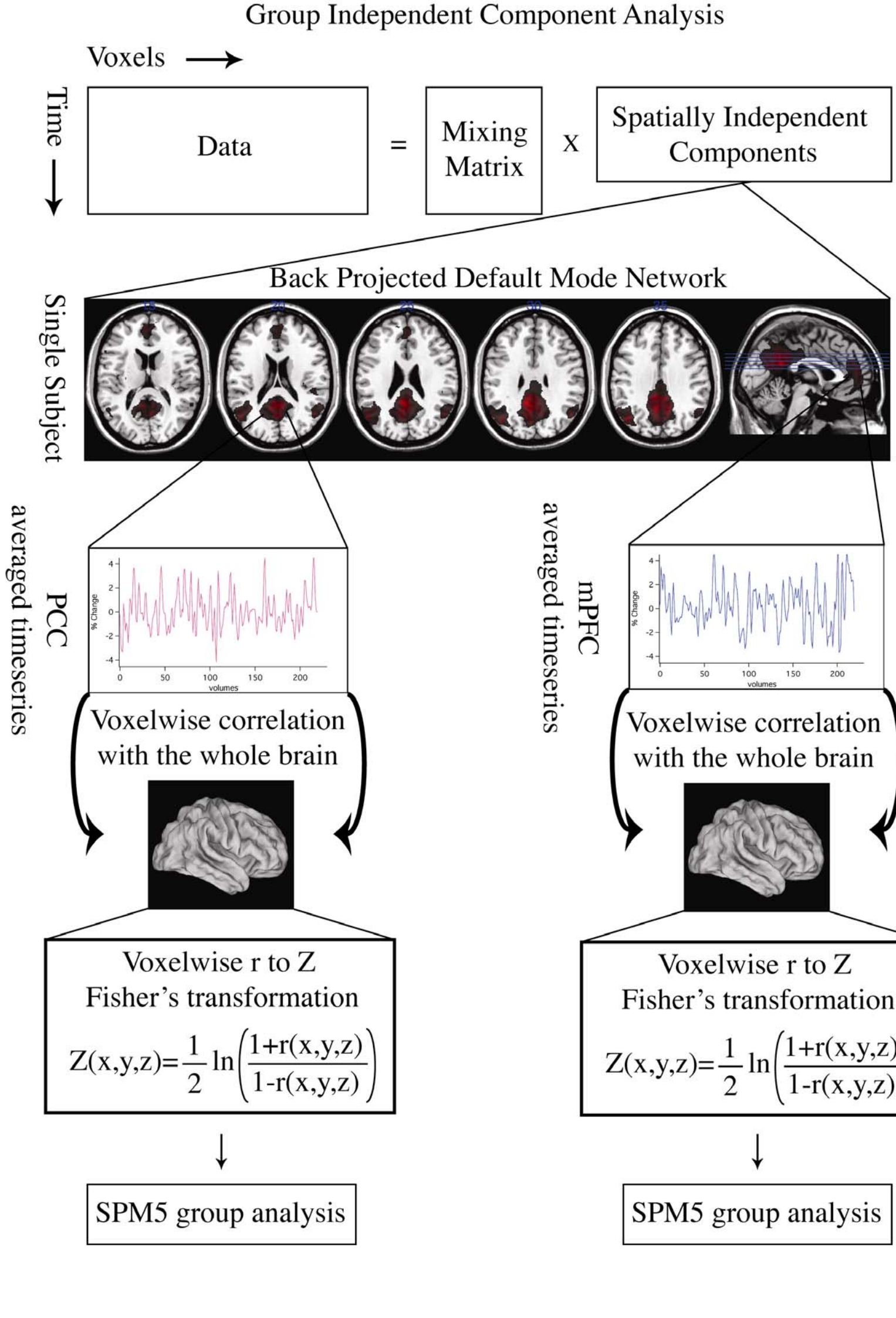
Group Independent Component Analysis
Voxels
Time
Data
=
Mixing Matrix
x
Spatially Independent Components
Back Projected Default Mode Network
Single Subject
PCC
averaged timeseries
% Change
volumes
Voxelwise correlation with the whole brain
mPFC
averaged timeseries
% Change
volumes
Voxelwise correlation with the whole brain
Voxelwise r to Z Fisher's transformation
$Z(x,y,z)=\frac{1}{2}\ln\left(\frac{1+r(x,y,z)}{1-r(x,y,z)}\right)$
Voxelwise r to Z Fisher's transformation
$Z(x,y,z)=\frac{1}{2}\ln\left(\frac{1+r(x,y,z)}{1-r(x,y,z)}\right)$
SPM5 group analysis
SPM5 group analysis

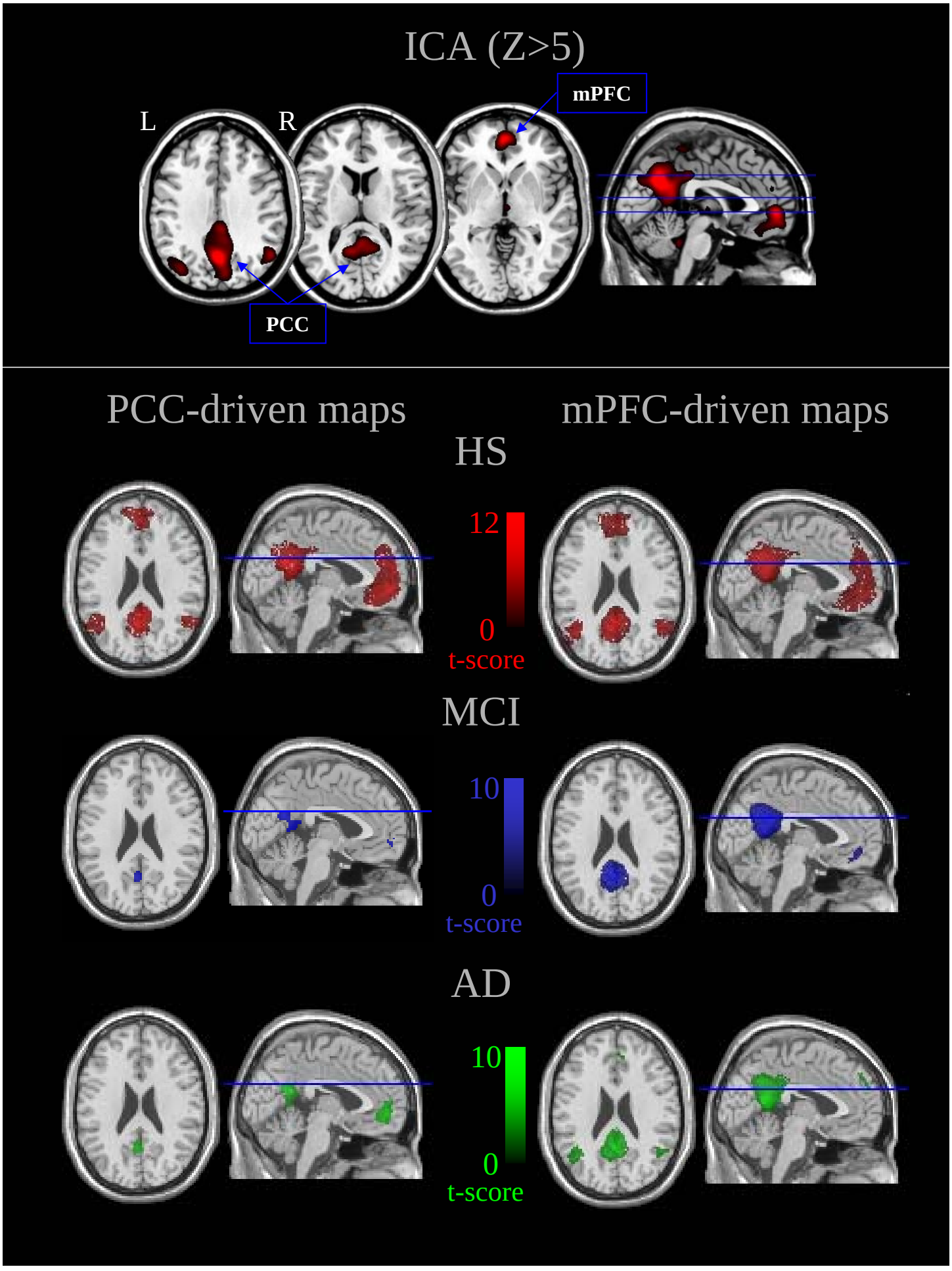
ICA (Z>5)
L
R
mPFC
PCC
PCC-driven maps
mPFC-driven maps
HS
12
0
t-score
MCI
10
0
t-score
AD
10
0
t-score

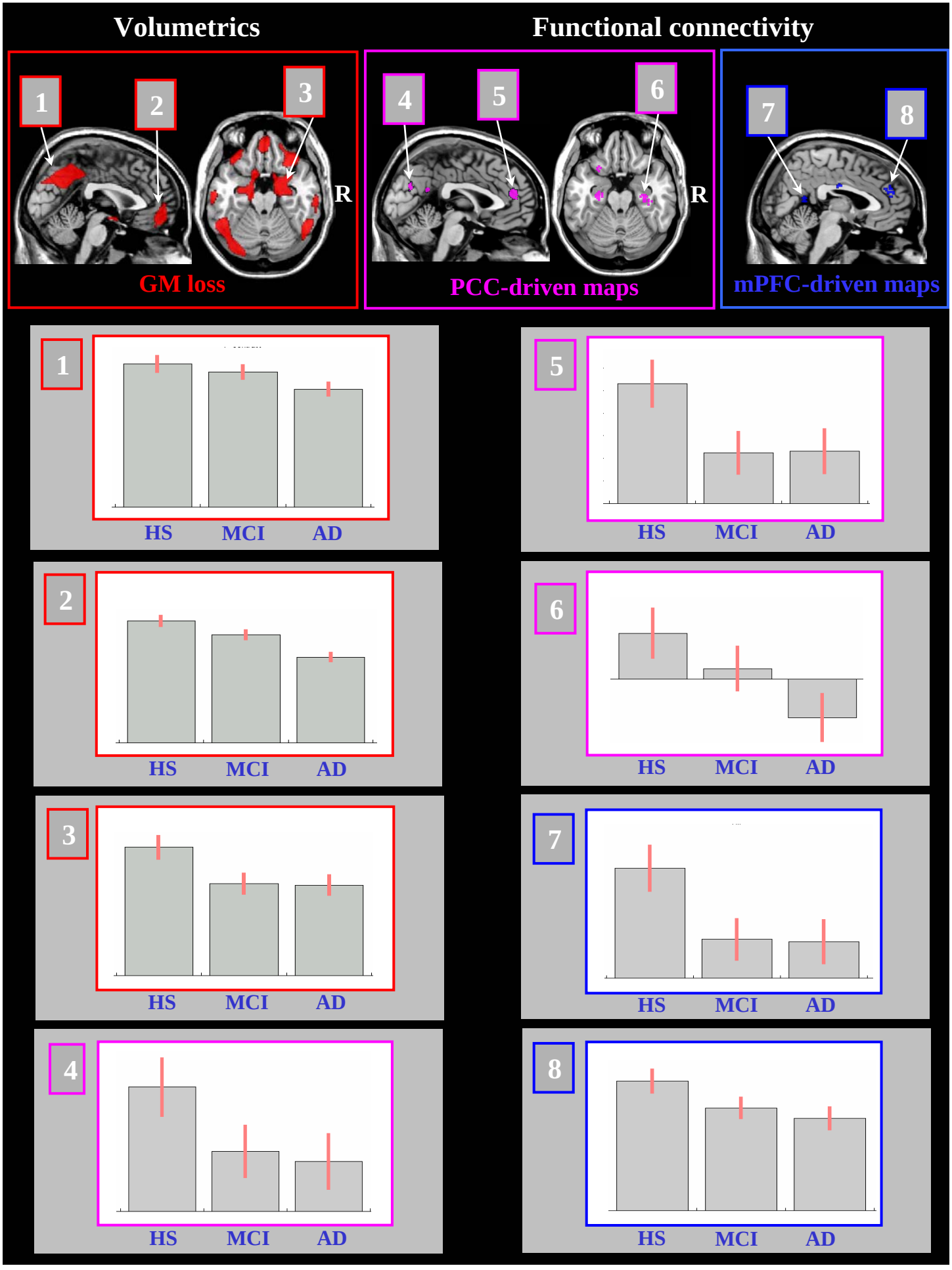
Volumetrics
Functional connectivity
1
2
3
R
GM loss
4
5
6
R
PCC-driven maps
7
8
mPFC-driven maps
1
HS
MCI
AD
2
HS
MCI
AD
3
HS
MCI
AD
4
HS
MCI
AD
5
HS
MCI
AD
6
HS
MCI
AD
7
HS
MCI
AD
8
HS
MCI
AD